Transactions, SMiRT-25
Charlotte, NC, USA, August 4-9, 2019
Division III

IMPACT ASSESSMENT ON LOCAL DAMAGE TO REINFORCED CONCRETE PANELS BY DIFFERENT PROJECTILES - IMPACT BEHAVIOR FOR PROJECTILES WITH HEMISPHERICAL NOSE SHAPE -

Zuoyi Kang[1], Minoru Nagai[2], Akemi Nishida[3], Haruji Tsubota[1] and Yinsheng Li[4]

[1] Researcher, Japan Atomic Energy Agency, Japan
[2] Visiting Researcher, Japan Atomic Energy Agency, Japan
[3] Senior Principal Researcher, Japan Atomic Energy Agency, Japan
[4] Group leader, Japan Atomic Energy Agency, Japan

ABSTRACT

Many empirical formulae have been proposed for evaluating the local damage to reinforced concrete (RC) structures caused by rigid projectile impact. The majority of these formulae were based on impact tests perpendicular to target structures, while few impact tests oblique to the target structure have been studied. The final objective of this study is to propose a new formula for evaluating the local damage to RC structures caused by oblique impact based on experimental and simulation results, Up to now, we validated the analytical method by comparison with the experimental results and conduct the simulation analysis of impact assessment on RC panel by rigid/soft projectile with flat nose shape using the validated analytical approach (Nishida et al., 2018). In this paper, the same analytical method is used to simulate the local damage to RC panels caused by oblique impact of rigid/soft projectile with hemispherical nose shape. The results associated with energy contribution ratio, time history of residual velocity etc. are presented.

INTRODUCTION

On the basis of the experience of the Fukushima nuclear power plant (NPP) accident, new regulatory requirements were published by NRA Japan to ensure the safety of NPP under various external events. The Japan Atomic Energy Agency (JAEA) has initiated a research on impact assessment for nuclear facilities caused by tornado, airplane attack, etc., to enable realistic evaluation for structural integrity and to enhance it.

Structural damage to reinforced concrete (RC) structures caused by a projectile impact includes local damage and an overall dynamic structural response. Impacting projectiles can be classified as either rigid or soft, depending upon whether the deformability of the projectile is small or large relative to the deformability of the target structure. The deformation of the projectile is more significant than the deformation of the target structure for a soft projectile, whereas rigid projectiles primarily affect the impact zone and cause local failure of the target structure, such as cracks, penetration, and perforation. In general, the local impact effects of an RC structure subjected to a rigid projectile (non-deformable projectile) include penetration, cone cracking, crack formation, spalling, scabbing, and perforation.

In addition, there are a few studies on the impact of soft projectiles in the literature. For example, the NEA/CSNI/IRIS_2010/2012 Final Report (2010-2014) and impact experiments on aircraft engines by

Sugano et al. (1993a) are among the few experimental cases that have been published. Sugano et al. (1993b) proposed a new local damage evaluation method for the collision of an aircraft engine, which is a soft projectile, based on their aforementioned previous experimental results. Normal impact experiments on a RC panel using a soft projectile were reported by Koshika (1994). The experimental setup and soft projectile are shown in Figure 1. For evaluating the validity and applicability of the analytical method, verification analysis has been conducted by Nishida et al. (2018).

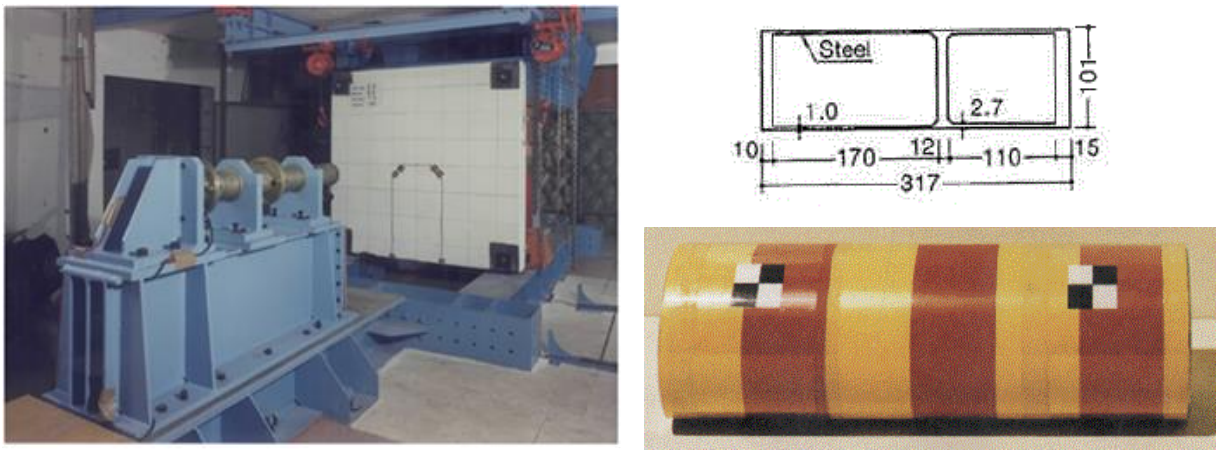

(a) (b)

Figure 1. (a) An experimental setup and (b) a soft projectile (unit: mm)

ANALYTICAL METHOD

The finite element code LS-DYNA R7.1.2 is used to perform the numerical analysis by adopting Lagrangian finite elements and explicit time integration. So far, through analysing impact assessment on RC panel by projectile with flat nose shape, results of reduction coefficient with respect to soft/rigid projectile and $0^{\circ}/45^{\circ}$ impact angle were obtained. The results of previous studies have suggested that nose shape of projectile greatly affect the damage to the RC structure. Therefore, as the next step, we planned to evaluate the influence of the difference in nose shape of projectile on the damage of RC structure. At first, we conducted analytical studies using a hemispherical nose shape of projectile that is expected to obtain standard results about the influence of the collision angle

FINITE ELEMENT MODELING

Reinforced Concrete Panel

The dimension of FE model of target RC panel in this simulation is the same with experimental specimen which is designed as 1500mm square plate with a thickness of 210 mm. The RC panel was fixed at its four corners, and anchor plates were attached at four fixed points on both faces of the target panel. The two corresponding anchor plates were connected by 30-mm-diameter steel pipes. As shown in Figure 2, the finite element model of the RC panel consists of concrete modelled by solid elements and steel rebar modelled by beam elements. The anchor plates and the steel pipes attached at the four corners were modelled as shell and beam elements, respectively. For the boundary condition of the target RC panel, the steel pipe in this study was assumed as a rigid beam element, and six degrees of freedom of the steel pipe were completely restricted. The element size of the concrete model is set to approximately 10 mm; thus, the RC panel consists of 21 layers along the thickness direction. A single node was used to connect the solid elements of the concrete and the beam elements of the rebar, ensuring a perfect bond between the concrete and the steel reinforcing bars. The symbol @ in Figure 2 means spacing of rebar. For example,

D6@40 means that D6 rebar is arranged with 40 mm pitch. The detailed information of RC model can be found in Table 1.

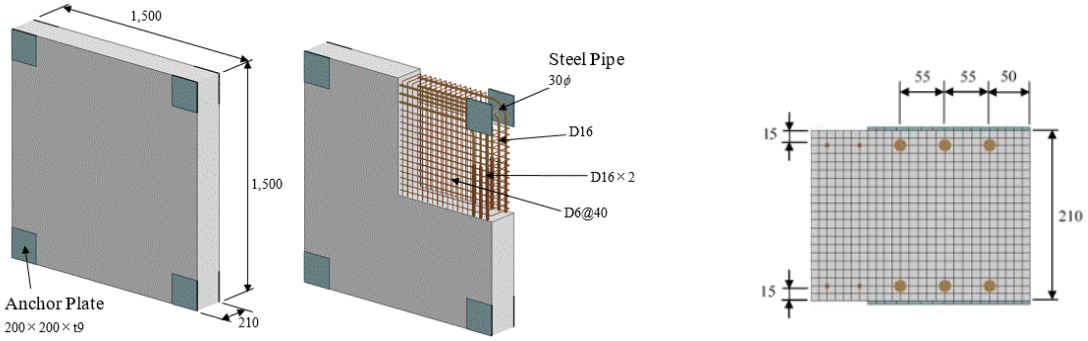

Figure 2. Target model (unit: mm)

Projectiles

Two types of projectiles are modelled in this research. The finite element (FE) model of each type is shown in Figure 3. The front nose of both two projectiles is hemispherical and the same mass is considered to investigate the influence of different projectile structures to local damage of RC panel. For the front component of rigid projectile and entire soft projectile, the same steel material is employed, whereas the rear part of rigid projectile is produced using aluminium material. Rigid projectile are modelled using solid elements, and the same node was used to connect the steel and aluminium components of the projectile. The soft projectile is modelled using solid elements for the front nose part and rigid frame parts and shell elements for the cylindrical body part. The total numbers of elements and nodes in the FE models of the soft and rigid projectile are summarized in Table 1.

For the FE formulation, reduced integration solid elements are used for the concrete and frame parts of the soft projectiles, in-plane four Gaussian points integration beam elements are used for steel rebar, and full integration shell elements are used for the other parts of the soft projectiles.

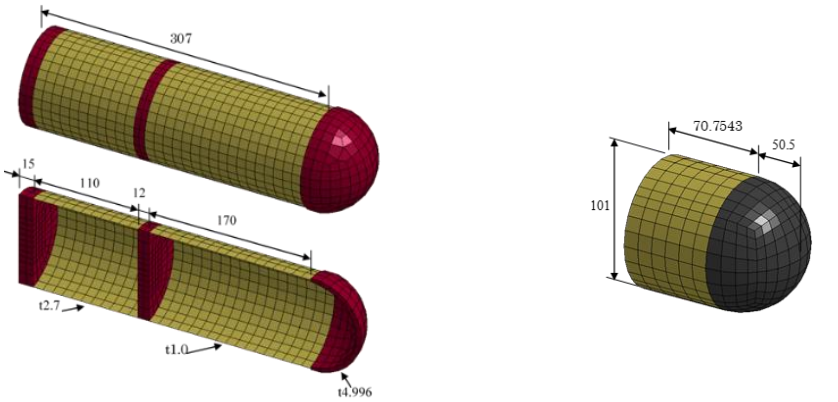

(a) soft projectile (b) rigid projectile

Figure 3. Projectile model (unit: mm)

Table 1: Total numbers of elements and nodes.

Model	Solid element	Shell element	Beam element	Node
RC panel	457,464	2728	21,028	485,606
Soft projectile	512	1072	-	1895
Rigid projectile	1408	-	-	1740

MATERIAL PROPETIES

Concrete

In this study, the concrete model was selected from the database of LS-DYNA and MAT_084, namely the Winfrith model, was used. The material properties of the concrete defined in the RC panel are listed in Table 2. In the impact analysis, the compressive/tensile strength and softening curve of the concrete model after impact may change in accordance with the strain rate dependency for each individual element in LS-DYNA. Because the strain rate effect of the concrete is automatically calculated in LS-DYNA, the dynamic increase factor is not applied to the compressive/tensile strength of the concrete.

Table 2: Material properties of concrete.

Compressive strength	MPa	24.517
Tensile strength	MPa	2.746
Mass density	t/mm^3	2.345×10^{-9}
Young's modulus	MPa	22,831
Poisson's ratio		0.2
Aggregate size	mm	10

Rebar

The material properties of rebars are listed in Table 3. D6 and D16 deformed rebars whose nominal diameters are 6 mm and 16 mm, respectively, were employed for the RC panel. The true stress–true strain relationship of the steel rebar is defined using an exponential function that passes the yield stress point and the maximum strength point, as illustrated in Figure 4. The strain rate effect was considered for the steel rebar by applying the WES formula defined in WES-2808 (WES 20808, 2003).

Table 3: Material properties of rebar.

	Unit	D6	D16
Mass density	t/mm3	7.86 × 10−9	7.85 × 10−9
Young's modulus	MPa	205,000	223,000
Yield stress	MPa	447.2	464.8
Nominal tensile strength	MPa	585.5	653.1
True tensile strength	MPa	685	764.2
True fracture strain	mm/mm	0.157	0.157
Fracture strain	mm/mm	0.2	0.2
Poisson's ratio		0.3	0.3

Projectiles

The S45C steel is adopted to assign the material properties to soft projectiles. The specific parameters of the material properties are listed in Table 4. The strain-rate effect is considered to be the same as that described in Figure 4.

Table 4: Material properties of soft projectile.

Mass density	t/mm3	8.136×10^{-9}
Young's modulus	MPa	214000
Yield stress	MPa	411.9
Nominal tensile strength	MPa	705.1
True tensile strength	MPa	846.1
True fracture strain	mm/mm	0.1906
Fracture strain	mm/mm	0.5
Poisson's ratio		0.3

SS400 steel and A5083 aluminium are utilized to model the material properties for the front and rear part of the rigid projectile, respectively. The specific material properties are listed in Table 5. An identical mass (3.6 kg) for both projectiles is required and the density of each component was adjusted slightly. The reason is that the kinetic energy of each projectile should keep constant influence on the precision of the impact analysis.

Table 5: Material properties of the rigid projectiles.

	Unit	Steel	Aluminium
Mass density	t/mm3	7.86×10^{-9}	2.7×10^{-9}
Young's modulus	MPa	214,000	72,000
Yield stress	MPa	411.9	195
Nominal tensile strength	MPa	705.1	345
True tensile strength	MPa	846.1	-
True fracture strain	mm/mm	0.1906	-
Fracture strain	mm/mm	0.5	-
Poisson's ratio		0.3	0.33

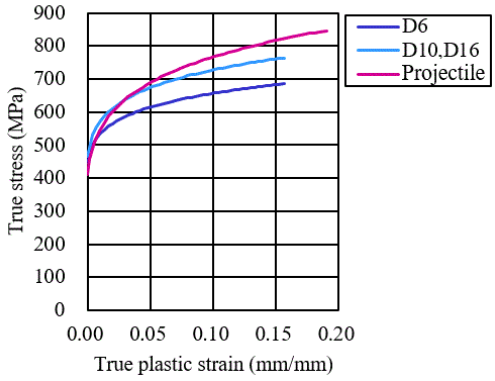

Figure 4. True stress–true strain relationship.

ANALYSIS CONDITIONS

Contact Conditions

In the simulation analyses, three types of contact conditions are defined between the projectile and the RC panel. The contact conditions and friction coefficients used in the analyses are summarized in Table 6. To determine the internal energy and resulting local damage of the RC panel, the number of ruptured elements in the RC model should be confirmed. Therefore, an eroding contact condition is set between the projectile and the concrete; thus, the ruptured elements that exceed the failure strain of the material during impact are

removed. All of these conditions are based on contact calculations performed using the penalty method.

Due to the differences in the element properties, the contact between the projectile and steel rebar is defined as contact between a solid element and a beam element in the simulation analysis. The node-to-surface contact condition can adequately represent the projectile–steel rebar contact. A single-surface contact is defined for the case in which the deformed projectile or a fragment of the ruptured projectile contacts itself. On the basis of these conditions, the contact calculations are implemented using the penalty method. In addition, the friction coefficient for each contact condition is not always known; thus, we adopted generic values that are widely used in contact calculations (Architecture Handbook, 1977).

Table 6: Definition of contact conditions.

Object	Contact condition	Friction coefficient
Projectile-concrete	eroding	0.3
Projectile-rebar	nodes to surface	0.2
Self-contact of projectile	single surface	0.2

Analysis Cases

In this work, four cases are investigated to verify the local damage of an RC panel subjected to normal and oblique impact by soft and rigid projectiles as summarized in Table 7. The graphical representation of the RC panel and projectile for each case just before the impact is shown in Figure 5.

Table 7: Cases of impact simulation analysis.

Case	Impact angle	Impact velocity	Projectile type
1	0°	201m/s	soft
2			rigid
3	45°		soft
4			rigid

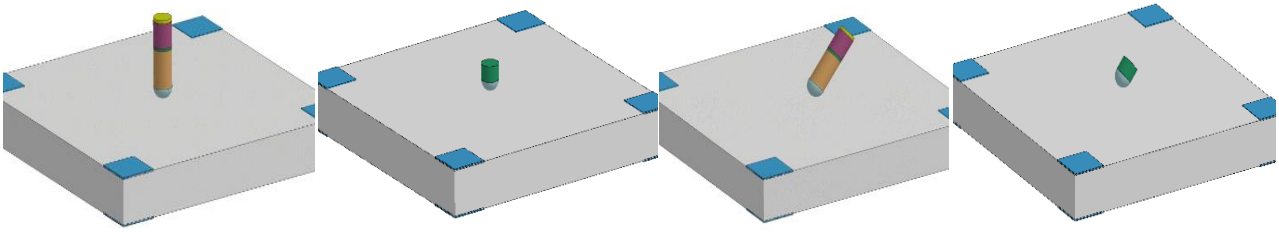

case 1 case 2 case 3 case 4

Figure 5. Illustration of the projectile and RC panel for each case.

NUMEIRCAL ANALYSIS

Impact Behaviours

The partial cross sections of RC panel and projectiles are illustrated in Figures 6 and 7. For the normal impact in Figure 6, both types of projectiles formed a cylindrical hole on the surface of RC panel due to hemispherical nose shape of projectile. The rigid projectile kept the penetrating state from t = 0 ms to t = 10 ms, whereas, the soft projectile was divided into two parts at t = 4 ms due to the rupture of shell component in the front of projectile. Moreover, the buckling of hemispherical nose of projectile occurred for soft projectile in normal impact. For oblique impact in Figure 7, the rigid projectile colliding with the RC specimen rebounded slightly, exhibiting rotational motion, and a conical damage zone was formed because of the incident angle. However, the soft projectile embedded into RC panel without rebounding.

The hemispherical nose of projectile was not collapsed and front shell part of projectile severely damaged. More complicated deformation mode was presented by comparison with that in normal impact. In addition, it is founded that there is no obvious deformation for each part of rigid projectile in normal and oblique impact. Furthermore, the surface damage depth, regarded as the maximum depth of the crater measured along the direction normal to the target surface, caused by the rigid projectile was larger than that caused by soft projectile for each case.

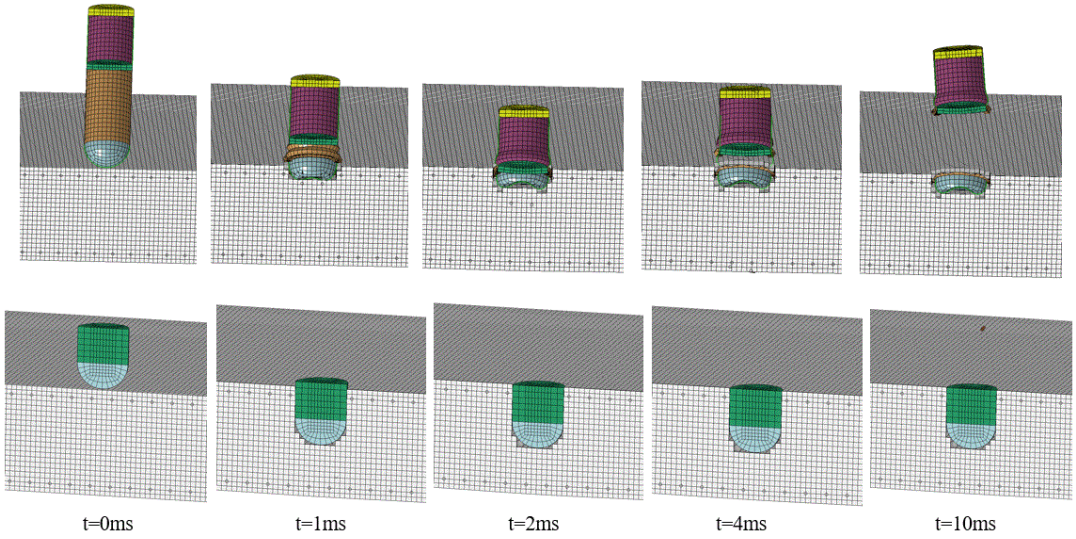

Figure 6. Interaction of projectile and RC panel for case 1 (upper) and case 2 (lower).

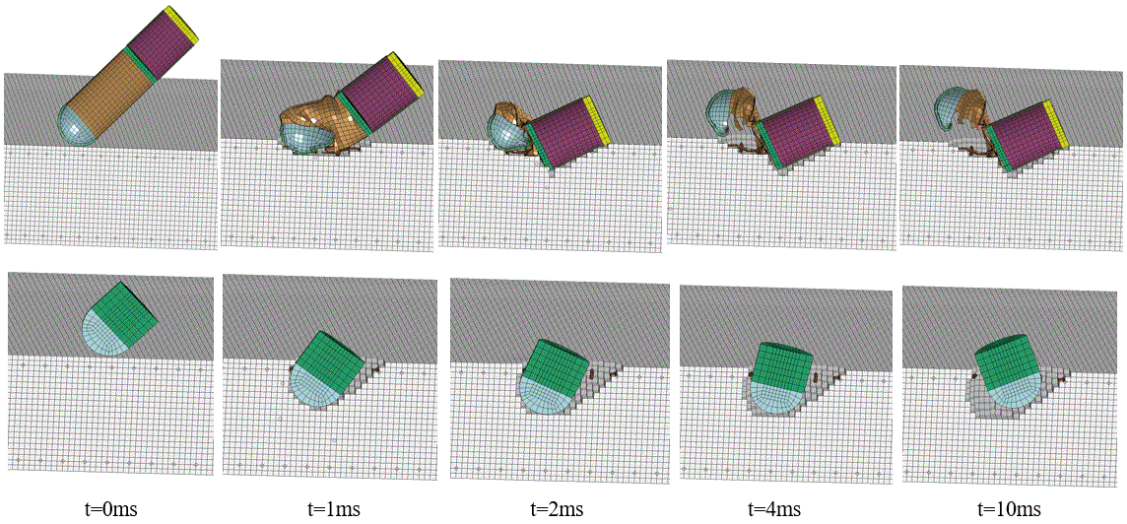

Figure 7. Interaction of projectile and RC panel for case 3 (upper) and case 4 (lower).

Energy Transmission

Because the energy transmission approximately become stable t = 3 ms, energy transmissions of RC panel and projectile during 3 ms after collision are shown in Figures 8-11. In Figure 8, the comparison of the time history of the internal energy of RC panel shows the final internal energy of RC panel for the rigid projectile is larger than that for the soft projectile, this consistence implies that the ruptured portion in the target RC panel due to impact of rigid projectile is larger compared to those observed under impact of soft projectile from the beginning. It can be found the maximum of local damage of RC panel can be obtained in the case of rigid projectile in oblique impact. The time history of kinetic energy of RC panel

for each case is illustrated in Figure 9. The results indicate that the kinetic energy of the RC panel becomes stable at approximately 0.8 ms, with no further increases for rigid projectile. However, the soft projectile impact consumed more time around 1.5-2 ms to make the RC panel keep stable. It is apparent that rigid projectile caused more kinetic energy of the RC panel by comparison with soft projectile.

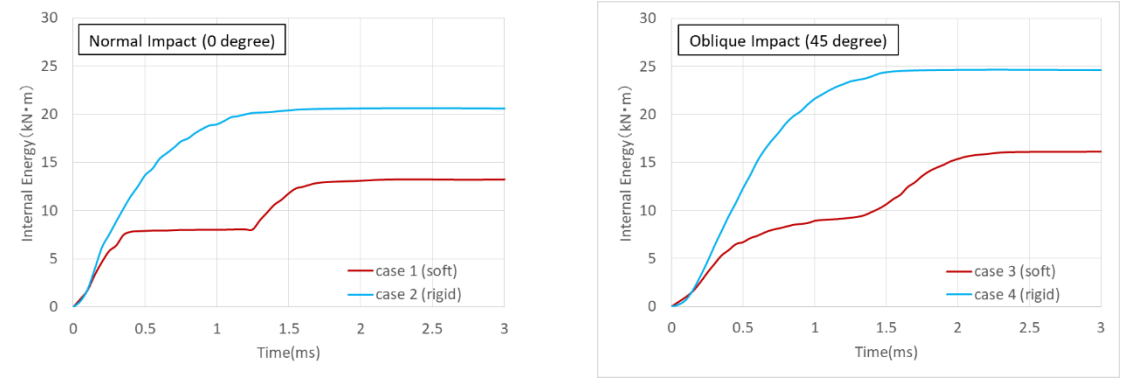

Figure 8. Time history of internal energy of RC panel for 0 degree (left) and 45 degree (right).

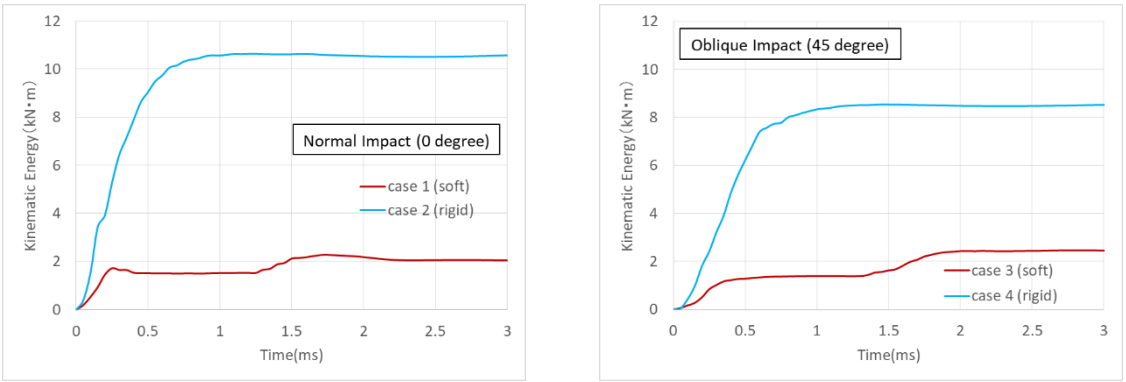

Figure 9. Time history of kinetic energy of RC panel for 0 degree (left) and 45 degree (right).

For the internal energy of projectiles, the larger internal energy of soft projectile was obtained compared with the rigid projectile as shown in Figure 10. The internal energy of soft projectile for normal impact is approximately 1.5 times larger than that of soft projectile for oblique impact due to the more serious rupture occurred for soft projectile in normal impact. Figure 11 shows that the rigid projectile's kinetic energy was consumed by 1.5 ms, while the kinetic energy of soft projectile was consumed by 1.7 ms for normal impact and by 2.4 ms for oblique impact, respectively. The results demonstrate that the kinetic energy of the rigid projectile decreased more rapidly than that of the soft projectile.

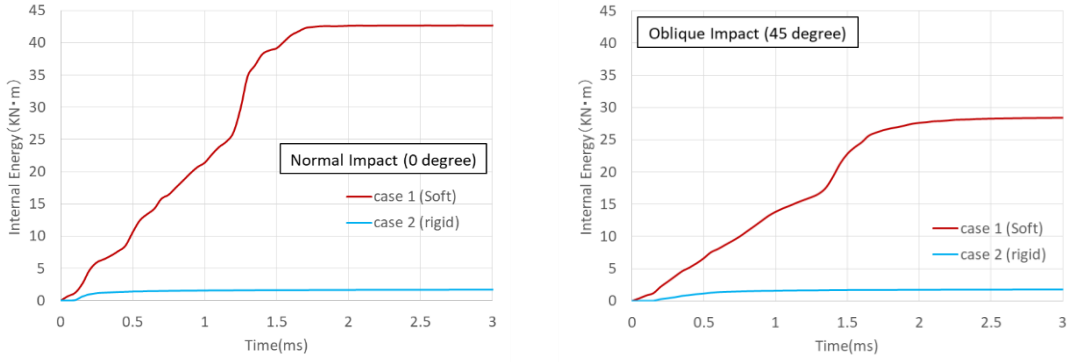

Figure 10. Time history of internal energy of projectile for 0 degree (left) and 45 degree (right).

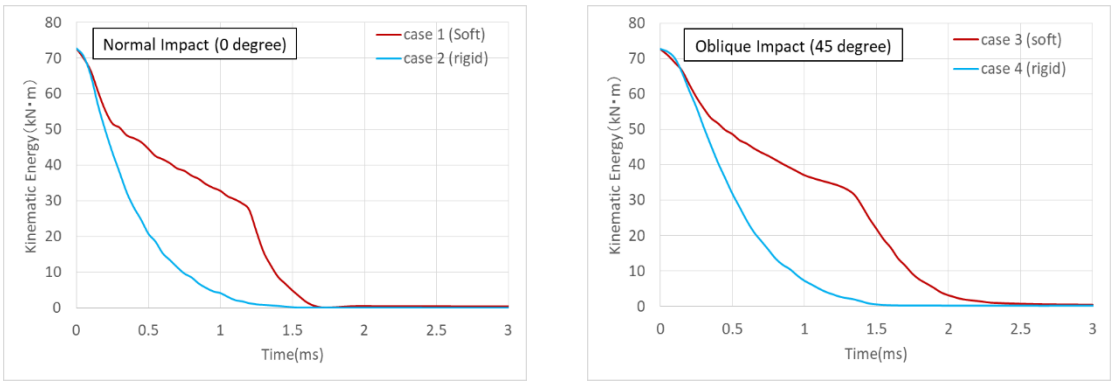

Figure 11. Time history of kinetic energy of projectile for 0 degree (left) and 45 degree (right).

Energy Contribution ratio

Subsequently, the energy contribution ratio for each case was calculated. First, the definitions of the following parameters are presented:
KE: Kinetic energy
IE: Internal energy
Sliding energy: Energy consumed due to friction.

The energy contribution ratios for each impact case at t = 3 ms are illustrated in Figure 12. The results show that the sliding energy and the internal energy of the RC panel are dominant compared with the other forms of energy in the impact of rigid projectile. However the internal energy of projectile and sliding energy occupied a large proportion to total energy consumed in the impact process for soft projectile. As a result of aforementioned description, the buckling of hemispherical nose of projectile occurred in normal impact case, which results in more internal energy of projectile by comparison with the internal energy consumed by oblique impact as shown in Figure 12.

In addition, time histories of the velocity change for each case are shown in Figure 13. Obvious velocity oscillations can be found for rigid projectile and the velocity of the rigid projectile decreases more rapidly compared with the velocity of the soft projectile for normal and oblique impact. The gradual velocity change can be observed during the process of impact for rigid projectile as a whole. Moreover, the velocity approached to zero around 1.5 ms and the change rate becomes relatively stable. On the other hand, the bilinear velocity change appeared in the case of soft projectile impact for normal and oblique impact, which can be explained by the influence of different stiffness of soft projectile's component parts. For normal impact, the velocity of soft projectile approached to zero at approximately t = 1.7 ms. Comparably, the velocity of soft projectile is close to zero over t = 2.1 ms for oblique impact.

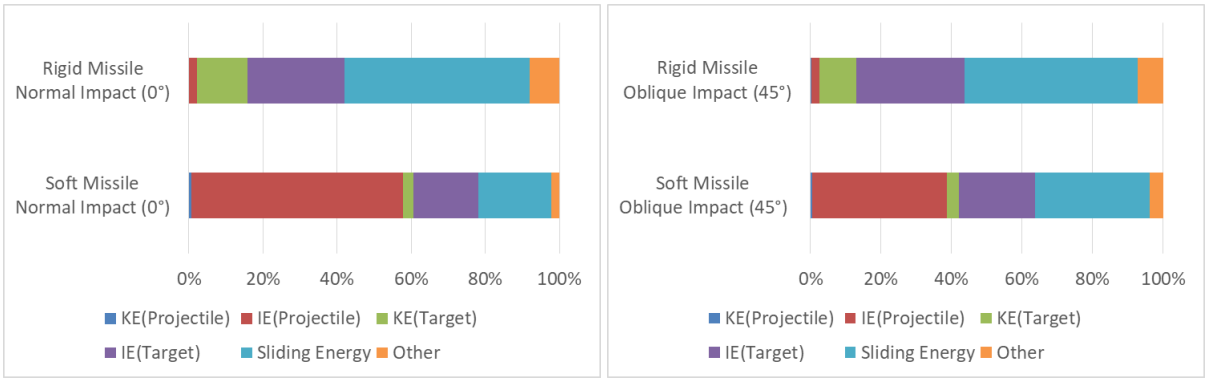

Figure 12. Energy contribution ratio for 0 degree (left) and 45 degree (right).

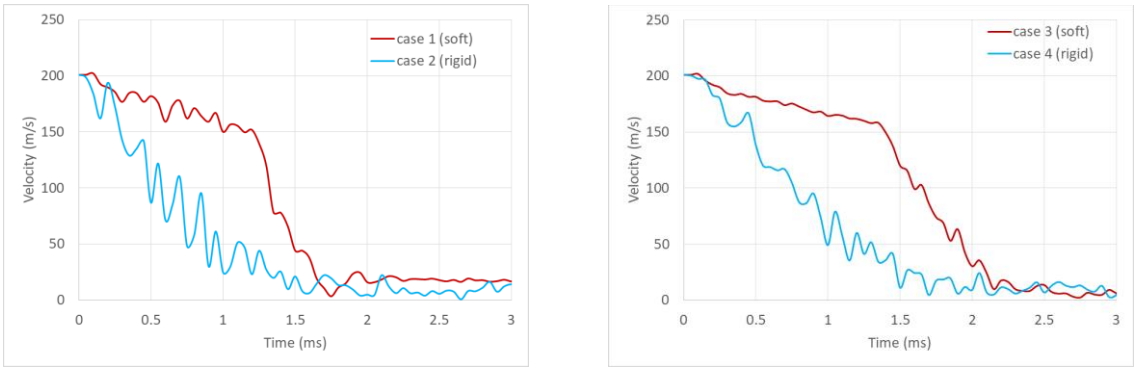

Figure 13. Velocity change for 0 degree (left) and 45 degree (right).

CONCLUSION

In this work, local damage to RC panels caused by soft/rigid projectiles with hemispherical nose shape was investigated by the validated analytical approach. According to the comparison of analytical results, the influence of different projectiles to the local damage of RC panels caused by normal and oblique impact was studied.

It is found that the local damage of RC panels caused by the rigid projectile is larger than that caused by soft projectile for normal and oblique impact. For the soft projectiles, more internal energy of soft projectile was consumed compared with the rigid projectile and the internal energy of soft projectile for normal impact is approximately 1.5 times larger than that of soft projectile for oblique impact. Furthermore, it is implied that the impact duration of soft projectile was longer than that of rigid projectile for normal and oblique impact. According to the results of energy contribution ratio, it is indicated that the sliding energy consumed by rigid projectile is larger than that consumed by soft projectile due to the deformation of projectile. Based on these achievements, the future work of this research is to investigate the influence of different nose shapes of projectiles to local damage of RC panel under oblique impact.

REFERENCES

Architecture Handbook II – Structure -, 2nd edition, (1977). Maruzen. (in Japanese)

Koshika, N. (1994). "A study on local damage of concrete structures subjected to impact loads," (in Japanese).

Nishida, A., Nagai, M., Tsubota, H. and Yinsheng, L. (2018). "Evaluation of local damage to reinforced concrete panels subjected to oblique impact – Simulation analysis for evaluating perforation phenomena caused by oblique impact of deformable projectiles –", *Mechanical Engineering Journal*, Japan, Vol.5, No.5.

OECD/NEA. (2010-2014). "Improving robustness assessment methodologies for structures impacted by missiles (IRIS_2010, IRISI_2012)," *Final report of IRIS2010, IRIS2012*, NEA/CSNI/R.

Sugano, T., Tsubota, H., Kasai, Y., Koshika, N., Ohnuma, H., Riesemann, W. A., Bickel, D. C. and Parks, M. B. (1993a). "Local damage to reinforced concrete structures caused by impact of aircraft engine missiles Part 1. Test program, method and results," *Nuclear Engineering and Design*, UK, 140 387-405.

Sugano, T., Tsubota, H., Kasai, Y., Koshika, N., Itoh, C., Shirai, K., Riesemann W. A. V., Bickel, D.C. and Parks, M. B. (1993b). "Local damage to reinforced concrete structures caused by impact of aircraft engine missiles Part 2. Evaluation of test results," *Nuclear Engineering and Design*, UK, 140, 407-423.